Research Paper

Improving the Oral Absorption of Celecoxib *via* Solid Self-Microemulsion Drug Delivery System: Preparation and *In Vitro*/*In Vivo* Evaluation

XIN ZHANG, XIAOWEN WU, YINGSHU FENG[3], CALEB KESSE FIREMPONG[1], QUANZHU YANG, TIANXIANG CHEN, DONGLI LI AND HONGFEI LIU[2,4]*

School of Biotechnology and Health Sciences, Wuyi University, Jiangmen 529000, [1]College of Pharmacy, Jiangsu University, Zhenjiang 212013, [2]Jiangmen Hongxiao Biomedical Co., Ltd, Jiangmen 529000, [3]Zhenjiang Key Laboratory of Functional Chemistry, Institute of Medicine and Chemical Engineering, Zhenjiang College, Zhenjiang, 212028, [4]Jiangsu Sunan Pharmaceutical Industrial Co., LTD, Zhenjiang, 212400, China

Celecoxib is a specific cyclooxygenase-2 inhibitor with poor solubility and low bioavailability. A solid self-microemulsifying drug delivery system of celecoxib was therefore developed to improve *in vitro* drug solubility and *in vivo* absorption. Solubility testing, compatibility testing and pseudo-ternary phase diagrams were employed in the design. Morphological observation, droplet size and *in vitro* release were used to characterize the formulation. The optimized celecoxib-liquid self-microemulsifying drug delivery system was determined as 10 % of celecoxib, 25 % of medium chain triglycerides, 56.25 % of emulsifier and 18.75 % of Transcutol HP. 3-[4,5-dimethylthiazol-2-yl]-2,5 diphenyl tetrazolium bromide assay was used to investigate the cytoxicity of active pharmaceutical ingredients, blank self-microemulsion and celecoxib liquid self-microemulsifying drug delivery system on Caco-2 cells. Celecoxib solid self-microemulsifying drug delivery system was prepared with Neusilin-US2 as a solid adsorbent and characterized using scanning electron microscopy, X-ray, Fourier-transform infrared spectroscopy, differential scanning calorimetry and *in vitro* release. Celecoxib liquid self-microemulsifying drug delivery system had a clear and transparent light-yellow appearance with average particle size of about 22.68 nm, zeta potential of -31.92 mv, and polydisperse coefficient of 0.141. 3-[4,5-dimethylthiazol-2-yl]-2,5 diphenyl tetrazolium bromide results showed that the formulations virtually had no cytotoxic effect on the cells. The results also showed that celecoxib existed in an amorphous state in celecoxib-solid self-microemulsifying drug delivery system, and the celecoxib-liquid self-microemulsifying drug delivery system and celecoxib-solid-self-microemulsifying drug delivery system had a dissolution degree of more than 90 % in different media with good stability. The pharmacokinetic studies showed that the area under curve of the liquid self-microemulsifying drug delivery system and self-microemulsifying drug delivery system increased by 6.59 and 6.37 folds, respectively, compared with celecoxib suspension. The findings showed that the developed solid self-microemulsion formulations improved the bioavailability of the drug with no cytotoxicity, hence the formulation can serve as a promising carrier for the oral delivery of celecoxib.

Key words: Celecoxib, self-microemulsion drug delivery system, solid adsorption, bioavailability

Celecoxib (CXB), a non-steroidal anti-inflammatory drug, is classified as a highly selective Cyclooxygenase-2 (COX-2) inhibitor. COX-2 inhibitors have the selectivity for up to hundreds of times and can effectively treat inflammation while avoiding or reducing the adverse effects caused by inhibition of COX-1[1]. The phenyl group of CXB binds to the hydrophobic channel of COX-2, and the hydrophilic sulfonamide group forms a hydrogen chain with arginine at position 513 and histidine at position 90 in the "side pocket" of COX-2, and can closely bind to arginine at position 120 of

***Address for correspondence**
E-mail: liuhongfei2000@163.com

Accepted 01 November 2023
Revised 23 October 2023
Received 11 April 2023
Indian J Pharm Sci 2023;85(6):1821-1838

COX-2 to inhibit the production of prostaglandins. The CXB has high anti-inflammatory, analgesic and anti-tumor activities, with high targeting, few side effects, good tolerability and safe use which provide evidence for its clinical advantages[2]. As reported elsewhere, CXB has been successfully used to treat breast cancer[3].

CXB was approved by the FDA in 1999 and Celebrex® is an orally available product of CXB capsule developed by Pfizer for the treatment of rheumatoid arthritis. CXB belongs to class II drugs of the biopharmaceutical classification system with low water solubility (only 3-7 mg/ml, at 20°) [2], which usually results in low bioavailability (only 30 %). Studies have also shown that the bioavailability of Beagle Dog Oral CXB capsules was only 30 % and the drug absorption was limited by the rate of dissolution[4]. Generally, the poor water solubility and low bioavailability greatly affect the *in vivo* pharmacodynamic effects of CXB. So far, several formulations have been adopted to overcome the low oral bioavailability of CXB, such as solid dispersions[5], liposomes[6], and so on. However, the dispersion state of the drug in the solid dispersion is not stable, and the long-term storage is also prone to aging[7]. Liposome stability is also poor, and easy to clump and fuse during storage[8]. Therefore, it has become urgent to develop new formulations to improve CXB solubility and bioavailability.

The Self-Microemulsion Drug Delivery System (SMEDDS) is a thermodynamically stable system composed of drugs, oil phase, emulsifiers and co-emulsifiers, which can form oil-in-water (O/W) Microemulsions (ME) with a particle size of less than 100 nm after slight stirring and oral administration through gastrointestinal peristalsis at room temperature, which can provide a large surface area for drug absorption, and then digested by various digestive enzymes and bile salts in the small intestine[9]. In addition, it can stimulate the gastrointestinal tract to produce lipoproteins and chylomicrons, stimulate lymphatic transport, increase the bypass transport of drugs, avoid first-pass metabolism in the liver, and indirectly improve the bioavailability of drugs[10]. SMEDDS can improve the solubility and bioavailability of lipophilic drugs, reduce the frequency of administration, avoid first-pass metabolism, and bypass P-glycoprotein efflux[11]. Consequently, SMEDDS technology has been applied to a series of drugs, such as Ibuprofen[12], Nintedanib[13], and Tacrolimus[14] with enhanced absorption. In addition, SMEDDS has a controlled-release and targeting effect as a carrier, using SMEDDS, sugar[15], sugar nanoparticles[16], hyaluronic acid[17], hydrogels, microspheres and micelles[18,19] as drug delivery carriers and surface modification, which greatly improved the targeting of drug delivery and had been widely used in liver targeting, brain targeting and lung targeting. Silberstein *et al.*[20] designed as an acute, low-dose, oral-solution SMEDDS formulation of CXB, increasing drug absorption and bioavailability of lipophilic drugs, which allows the use of lower doses with improved PK profiles without compromising efficacy and can be used to treat migraine headaches acutely. However, traditional SMEDDS is usually encapsulated in soft gelatin capsules, and Liquid-SMEDDS (L-SMEDDS) can interact with the capsule shell when stored for a long time, causing leakage, and is not suitable for the development of sustained-release dosage forms[9]. In addition, L-SMEDDS has low storage stability and limited shelf life. L-SMEDDS is filled in soft capsules or sealed in hard capsules, which is more expensive to produce.

Therefore, the delivery system can be prepared into a Solid-SMEDDS (S-SMEDDS) by solid adsorption and other methods to solve the aforementioned problem. The water-soluble and insoluble carrier materials, such as anhydrous dicalcium phosphate, mannitol, colloidal silica, and aluminum magnesium silicate was converted into S-SMEDDS using spray drying, freeze drying, solid carrier adsorption and other technologies to prepare pellets, powders or other solid dosage forms, which can be filled in capsules or pressed into tablets[21-23]. S-SMEDDS has some potential advantages in addition to the benefits of L-SMEDDS (improved drug solubility and oral bioavailability), such as improved stability/shelf life; patient acceptability; easy manufacturing; and economical packaging and transport[24]. Schmied *et al.*[25] published a study on the adsorption of novel cellulose-based microparticles as adsorptive carriers to convert CXB-L-SMEDDS to CXB-S-SMEDDS. The new cellulose-based microparticles were prepared by spray drying an aqueous dispersion containing Diacel® 10 and methylcellulose or gum arabic as binders, and the prepared CXB-S-SMEDDS did not change the drug release rate and degree of

L-SMEDDS, and was stable and could be stored for a long time. However, the preparation process was cumbersome, time-consuming, and the production cost was high. *In vivo* pharmacokinetic studies were not conducted.

This study was aimed at preparing CXB-loaded S-SMEDDS to improve the dissolution and oral bioavailability of the drug. The road map for the preparation of drug carriers was shown in fig. 1. CXB-loaded L-SMEDDS was optimized and then converted into solid form by solid carrier adsorption using magnesium aluminum silicate (Neusilin-US2) as the adsorption carrier. Neusilin-US2 has a very large specific surface area, which helps to adsorb oily excipients very efficiently using simpler granulation techniques[26]. Finally, the developed CXB-loaded S-SMEDDS were evaluated *via* morphological observation, droplet size, X-Ray Diffraction (XRD) analysis, Fourier-transform infrared spectroscopy (FT-IR), Differential Scanning Calorimetry (DSC), stability, *in vitro* release and pharmacokinetic evaluations.

MATERIALS AND METHODS

Materials:

CXB (≥99 %) was purchased from Dijia Pharmaceutical Group Co., Ltd (People's Republic of China). Medium Chain Triglycerides (MCT), Ethoxylated hydrogenated castor oil (RH 40) and Cremophor EL (EL 35) were obtained from BASF (Germany). Neusilin-US2, Neusilin-UFL2, and anhydrous dicalcium phosphate were obtained from Shanghai Changwei pharmaceutical excipients Co., Ltd (People's Republic of China). Aerosil®200 Pharma and Aerosil®300 Pharma were obtained from Evonik (Germany). SYLOID®244 FP was obtained from Beijing Fengli seeks medicine Co., Ltd (People's Republic of China) while all other chemicals, reagents and solvents were obtained from Sinopharm Group Chemical Reagent Co., Ltd (People's Republic of China).

Animals:

Fifteen male Sprague-Dawley rats (weighing 200~220 g) were obtained from the Experimental Animal Center of Jiangsu University, with a qualification certificate number of No. 202281822 and experimental ethics number UJS-IACUC-2022121902. All the conditions of the animal studies were performed strictly according to the standard protocol approved by Jiangsu University Animal Center.

Methods:

Quantification of CXB: A High-Performance Liquid Chromatography (HPLC) system equipped with an Agilent G1311A Pump and Agilent G1314 detector was adopted in this study. The unitary C18 column (150×4.6 mm, 5 µm) was used. The mobile phase was composed of methanol/phosphate buffer of pH 6.8 at the ratio of 68:32. The column temperature was 40° with the detection wavelength set at 254 nm.

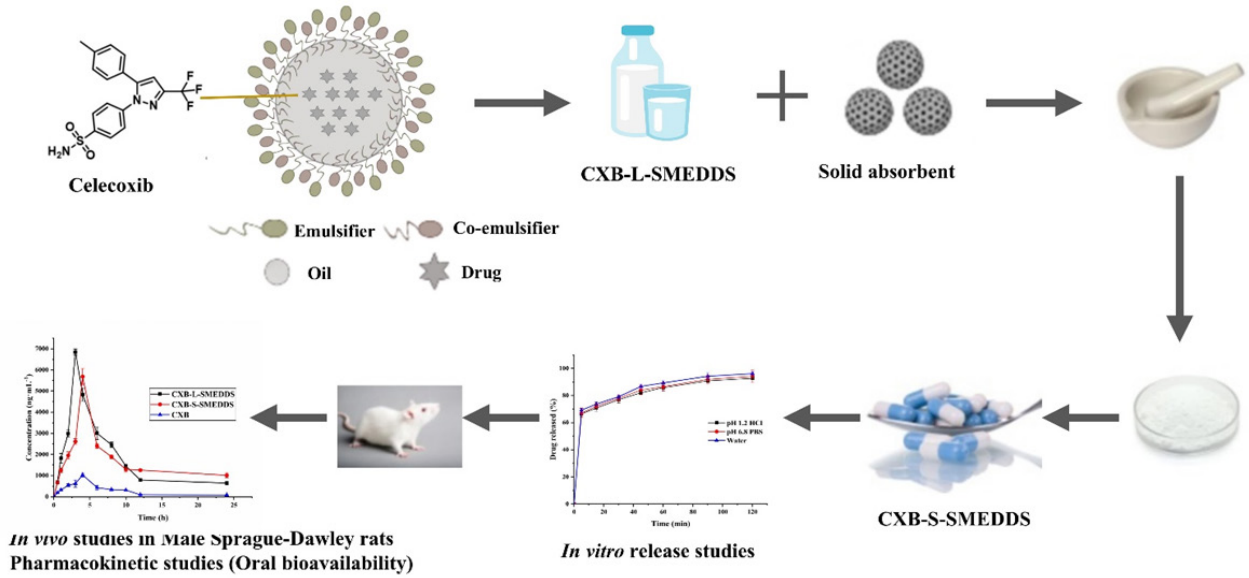

Fig. 1: The road map for the preparation of drug carrier

Optimization of the CXB-L-SMEDDS formulation:

Solubility testing of CXB in various accessories: Excessive CXB was added to a certain volume of oil phase, emulsifier, or co-emulsifier mixed with vortex and then stirred for 24 h at 37° in a constant temperature magnetic agitator (400 strokes per min) for equilibration. After that, the undissolved drug was separated by centrifugation at 10 000 rpm for 10 min. The solubility of CXB in different accessories was determined using an HPLC system after suitable dilution with methanol. All experiments were performed in triplicate.

Compatibility testing:

The oil phase (MCT, castor oil, oleic acid) and emulsifier (Cremophor RH40, Cremophor EL, Tween 80) were weighed at ratios of 1:9, 2:8, 3:7, 4:6 and 5:5 and mixed by vortexing. The mixture (0.5 g) was added to 50 ml of 37° water at 100 rpm with constant temperature magnetic stirring to form the ME. The ME was rated according to the visual grading system. There were five grades in the visual grading system, Grade A; rapid emulsification (≤1 min), clear or slightly pan-blue; Grade B; rapid emulsification (≤1 min), slightly clear, blue and white; Grade C; slower emulsification (≤2 min), bright white milk-like liquid; Grade D; slower emulsification (>2 min), dark gray, slightly oily appearance; Grade E; emulsifying difficulties or the existence of a large number of oil droplets.

Construction of pseudo-ternary phase diagrams:

CXB-L-SMEDDS was prepared by constructing pseudo-ternary phase diagrams, which were applied to confirm the optimal formula. Mixtures of oil phase (MCT, Castor oil), emulsifier (Cremophor RH40, Cremophor EL), and co-emulsifier (Transcutol HP) were prepared at weight ratios of 9:1 to 1:9, then put into 50 ml of 37° water at 100 rpm. The ME was graded by observing the formation and appearance according to the same aforementioned visual grading system. Based on the visual grade, the areas and boundary points where ME can be formed were determined, and a pseudo-ternary phase diagram was constructed.

Response surface method to optimize CXB-L-SMEDDS prescription:

Further optimization of CXB-L-SMEDDS prescription was performed using Central Composite Design (CCD). The CCD was used to investigate the influence of two independent variables, *viz.*, the mass fraction W (oil)(X_1) of the oil phase, and the mass ratio of the emulsifier and the co-emulsifier Km (X_2), on the light transmittance (T %) (Y). Experiments were carried out according to the 13 experimental protocols (including 4 cube points, 5 center points and 4 pivot points) designed using Design Expert 8.0.6 software. The 13 mixtures were weighed (1 g) and mixed by vertexing. The mixture (0.5 g) was added to 50 ml of 37° water at 100 rpm with constant temperature magnetic stirring to form the ME and the transmittance with an ultraviolet spectrophotometer at 550 nm was measured.

Preparation of CXB-L-SMEDDS:

With MCT as oil, Cremophor EL as emulsifier, Transcutol HP as co-emulsifier, Km as 3, MCT content of 25 %, and drug load of 10 %, CXB-L-SMEDDS was prepared in a water bath at 37° and stirred at 400 $r.min^{-1}$ for 30 min.

Characterization of CXB-L-SMEDDS:

Transmission electron microscopy and droplet size: The CXB-L-SMEDDS (0.5 g) was rapidly injected into 50 ml of distilled water using 100 rpm at 37°. The topography of CXB-L-SMEDDS was observed under Transmission Electron Microscopy (TEM). The droplet size and zeta potentials of CXB-L-SMEDDS were measured using zeta sizer Nano ZS90 particle size analyzer.

Thermodynamic stability:

CXB-L-SMEDDS were exposed to heat-cooling cycles (4° and 45°), freeze-thaw cycles (-21° and 25°) by exposing them to 3 cycles to assess their stability. Each storage cycle was not less than 48 h and the state of CXB-L-SMEDDS, self-emulsification to form the ME, were observed.

Effect of disperse media and dilution factor:

CXB-L-SMEDDS was diluted (1:50, 1:100, 1:200) in water and two different pH media (water, pH 1.2 and 6.8), and the emulsification time and light transmittance recorded. The samples were allowed to stand for 24 h to observe the stability of the ME and to check whether oil droplet coalescence, drug precipitation crystals or demulsification appeared.

Drug load and encapsulation rate of CXB-L-SMEDDS:

The Drug Load (DL) and Encapsulation rate (EE) calculation formulae of CXB-L-SMEDDS were as follows: (All experiments were performed in triplicate)

$DL\ (\%)=M_s/M_h\times100$ (1)

$EE\ (\%)=C_o\text{-}C_n/C_o\times100$ (2)

M_s was the actual measured drug content of CXB liquid from microemulsion, and M_h was the total amount of CXB liquid self-microemulsion; C_n represented the concentration of CXB not encapsulated in the formulation ($\mu g.ml^{-1}$), and C_o represented the total concentration of CXB in the formulation ($\mu g.ml^{-1}$).

Stability experiment of CXB-L-SMEDDS:

The CXB-L-SMEDDS samples were tightly sealed and placed in an environment of 4° and 30° for 60 d, accordingly. Afterward, the stability of CXB-L-SMEDDS was evaluated. The average particle size and drug content were assessed at 0 d, 30 d and 60 d.

Cytotoxicity study:

The cytotoxicity of CXB-L-SMEDDS to Caco-2 cells was evaluated using the 3-[4,5-dimethylthiazol-2-yl]-2,5 diphenyl tetrazolium bromide (MTT) assay method. Caco-2 cells were cultivated in culture medium supplemented with Fetal Bovine Serum ((FBS) 10 % v/v) containing penicillin/streptomycin (1 %, Gibco), in a CO_2 (5 %) and relatively humid (95 %) incubator at 37°. Caco-2 cells diluted to 1×10^5 ml^{-1} cell suspension were placed in 96-well cell culture plates and cultured for 24 h. Then, the medium was replaced with serum-free medium containing different concentrations of CXB solution (dissolved in dimethyl sulfoxide, containing 100 mg of CXB), CXB-SMEDDS (containing 100 mg of CXB), and blank SMEDDS. The blank and control groups were also set up and after 24 h, the cell viability was determined using an MTT assay. The absorbance value (OD) of each well was measured using a microplate reader at 490 nm. The relative viability of cells was calculated.

Formulation screening and optimization of CXB-S-SMEDDS:

Screening of solid adsorbent: CXB-L-SMEDDS was added dropwise to each of the solid adsorbent including anhydrous dicalcium phosphate, Neusilin-US2, Neusilin-UFL2, Aeroperl®300 Pharma, Aerosil®200 Pharma, mannitol, SYLOID®244 FP, povidone K30 and evenly mixed. The amount of CXB-L-SMEDDS was recorded as the maximum amount of adsorption as the first screening indicator when the sorbent began to wet. The *in vitro* release of CXB-S-SMEDDS at 60 min was used as the secondary screening indicator. Combined with adsorption and release capacity, the adsorbent type was screened out using a single factor test.

The mass ratios of the optimal sorbent (Neusilin-US2) to CXB-L-SMEDDS were set at 2.5:1, 2:1, 1.5:1, 1:1 to screen the amount of adsorbent. The CXB-S-SMEDDS Carr's Index (CI), Hausner Ratio (HR) and angle of rest were determined to examine the powder fluidity of the formulation. The rest angle was less than 30°, with the Hausner ratio less than 1.2 and the card index also between 15 %~25 %, which indicated that the compressibility and filling of the formulation were better[27]. The amount of sorbent was determined according to the powder fluidity, dissolution degree and microemulsion particle size formed by the CXB-S-SMEDDS.

Preparation of CXB-S-SMEDDS:

Physical adsorption was used to prepare CXB-S-SMEDDS. According to the ratio of CXB-L-SMEDDS:Neusilin-US2 (2:1), Neusilin-US2 was weighed and placed in a mortar. CXB-L-SMEDDS was slowly added to the sample and gently ground evenly until no large particles existed. The samples were placed in a 40° oven to dry, passed through a 60-mesh sieve to obtain CXB-S-SMEDDS powder. An appropriate amount of CXB-S-SMEDDS powder (containing 60 mg of CXB) was filled into 0# hollow hard capsule.

Characterization of CXB-S-SMEDDS:

Scanning Electron Microscopy (SEM): SEM was used to observe the surface structure of CXB, Neusilin-US2 and CXB-S-SMEDDS. The samples were individually placed on double-sided carbon conductive tape, fixed to a glass slide, and the powder that was not firmly attached with an ear wash ball blown off. Morphological features were observed at different magnifications.

Droplet size, polydispersity index and zeta potential: The CXB-S-SMEDDS (0.5 g) was rapidly injected into 50 ml of distilled water using 100 rpm at 37°. The droplet size and zeta potentials of CXB-S-SMEDDS were measured using zeta sizer Nano ZS90 particle size analyzer.

XRD: X-ray diffractometer was used to measure XRD of CXB, Neusilin-US2 and CXB-S-SMEDDS to analyze how drugs and excipients were bound. Samples were loaded into thin layers in a sample holder, and all the samples were scanned in steps of 0.02° in a range of 5°-85° with a tube voltage of 40 kV and a tube current of 30 mA.

FT-IR: FT-IR as a physical characterization of solid dosage forms was adopted, using the principle of diffuse reflection[23]. FT-IR spectra of CXB, Neusilin-US2 and CXB-S-SMEDDS powders were recorded using the KBr disc method (2 mg sample in 100 mg of KBr), and scanned in the range of 400-4000 cm^{-1}.

DSC: DSC was used to measure the melting point of the drug and to determine the crystal form of the drug in the preparation. CXB, Neusilin-US2 and CXB-S-SMEDDS, 20 mg each, were placed in an alumina crucible. A blank alumina crucible was used as a control and a differential scanning calorimeter was used for the experiment. The sample was purged with pure dried N_2 at a flow rate of 50 ml/min to raise the temperature to the range of 30-300° with a heating rate of 10.0 K/min.

Content of CXB-S-SMEDDS:

The CXB-S-SMEDDS (0.1 g) was weighed, placed in a volumetric flask, and diluted with methanol at an appropriate multiple. The content of CXB-S-SMEDDS was determined using an HPLC system. All experiments were performed in triplicate.

***In vitro* dissolution of CXB-S-SMEDD:**

Referring to the dissolution and release determination method in the 2020 edition of the Chinese Pharmacopoeia, the *in vitro* dissolution of CXB, CXB-L-SMEDDS and CXB-S-SMEDDS was determined using the basket method. Using HCl (pH of 1.2), Phosphate-Buffered Saline (PBS) (pH of 6.8) and water as the dissolution media, the experiment was performed at 37±0.5° with 900 ml of the sample at a speed of 50 rpm. After the experiment had started, the CXB (60 mg), CXB-S-SMEDDS capsule (containing 60 mg of CXB) and CXB-L-SMEDDS capsule (containing 60 mg of CXB) were put into the dissolution cups, timing started. The samples (5 ml of aliquot each) were collected at predetermined time intervals (5, 15, 30, 45, 60, 90 and 120 min) and the aliquots supplemented with fresh buffer (5 ml each). The sample solution was determined using an HPLC system. All dissolution experiments were performed in triplicate.

Stability of CXB-S-SMEDDS:

Stability study of CXB-S-SMEDDS was carried out for 6 mo (thus, at 1, 2, 3 and 6 mo) at 40±2°/75 % RH±5 % RH. These formulations were analyzed using appearance and the content of CXB in CXB-S-SMEDDS.

***In vivo* pharmacokinetic study:**

Male Sprague-Dawley rats (180-220 g) were fasted for 12 h (with free drinking access) before the experiment. The rats were randomly divided into three groups (n=5) and orally given CXB, CXB-L-SMEDDS and CXB-SMEDDS (CXB dose of 10 $mg.kg^{-1}$). Aliquot (0.5 ml each) of blood samples was taken from the orbit region at 0.5, 1.0, 1.5, 2.0, 3.0, 4.0, 6.0, 8.0, 10 and 12 h after the sample administration. The blood samples were centrifuged at 10 000 $r.min^{-1}$ for 10 min to collect the upper plasma. A quantity of plasma (200 µl) was withdrawn and added to 50 µl of the internal standard solution (100 $\mu g.ml^{-1}$ carbamazepine solution) and 750 µl of methanol. The sample mixture was then shaken for 2 min and centrifuged at 10 000 $r.min^{-1}$ for 10 min. A quantity of supernatant (20 µl) was also withdrawn and was determined using an HPLC system.

RESULTS AND DISCUSSION

CXB had the highest solubility (418.7±7.45 mg/g) in Transcutol HP as co-emulsifier probably due to the formation of the hydrogen bond between carbonyl from CXB and the hydroxyl from Transcutol HP (fig. 2), Therefore, the Transcutol HP was selected as a co-emulsifier to improve the solubility of CXB in the system and to stabilize the microemulsion for reducing the interfacial tension as reported by others[28]. The solubility of CXB in the oil phase (Castor oil, MCT, Oleic acid)

was also high, so these three types of oils were preliminarily selected as the oil phase. Solubility in emulsifiers varied widely, so it was screened using subsequent self-emulsifying grading test and pseudo-ternary phase diagrams.

The Oleic acid was rated D or E, which indicated that it was not compatible with most emulsifiers to form a stable and delicate microemulsions (Table 1). In contrast, MCT and Castor oil were compatible with some emulsifiers to form A or B grade, which meant that these formulations could display a clear or slightly blue opacification appearance after self-assembly in interacting with water. Therefore, the oil phase was determined by drawing a pseudo-ternary phase diagram. In addition, RH 40 and EL 35 had better compatibility with MCT and Castor oil than Tween 80, so the compatibility of RH 40 and EL 35 with the co-emulsifier Transcutol HP was investigated to determine whether they could be used to prepare self-microemulsion.

The area size of the pseudo-ternary phase diagram was related to the stability of the microemulsion system (fig. 3). The larger the area of the pseudo-ternary phase diagram, the better the stability of the microemulsion system[29]. Therefore, MCT (oil), Cremophor EL (emulsifier) and Transcutol HP (co-emulsifier) had the largest microemulsion area and were selected directly for further optimization.

The CCD method is a statistical tool used to optimize the effective statistical design of multifactorial experiments in formulation development to optimize the level of variables to achieve the best response[22]. The Design-Expert 8.0.6 software was used to analyze the data and subsequently obtain the appropriate model-fit (Table 2). The binomial equation was as follows:

$Y = 94.74 - 29.92X_1 + 19.28X_2 + 13.83X_1X_2 - 17.11X12 - 13.27X_2^2$ (R2=0.9572, p=0.0001)

X_1 was W (oil) while X_2 was the Km value. The model F-value was 31.44, which indicated that the model was significant, with only a 0.01 % probability that such a large "F-value model" will occur due to noise. A value of "prob>F" less than 0.0500 indicated that the model term was significant and there was no significant difference in the Lack of Fit term, which indicated that the model fitted with a central composite design had a high accuracy.

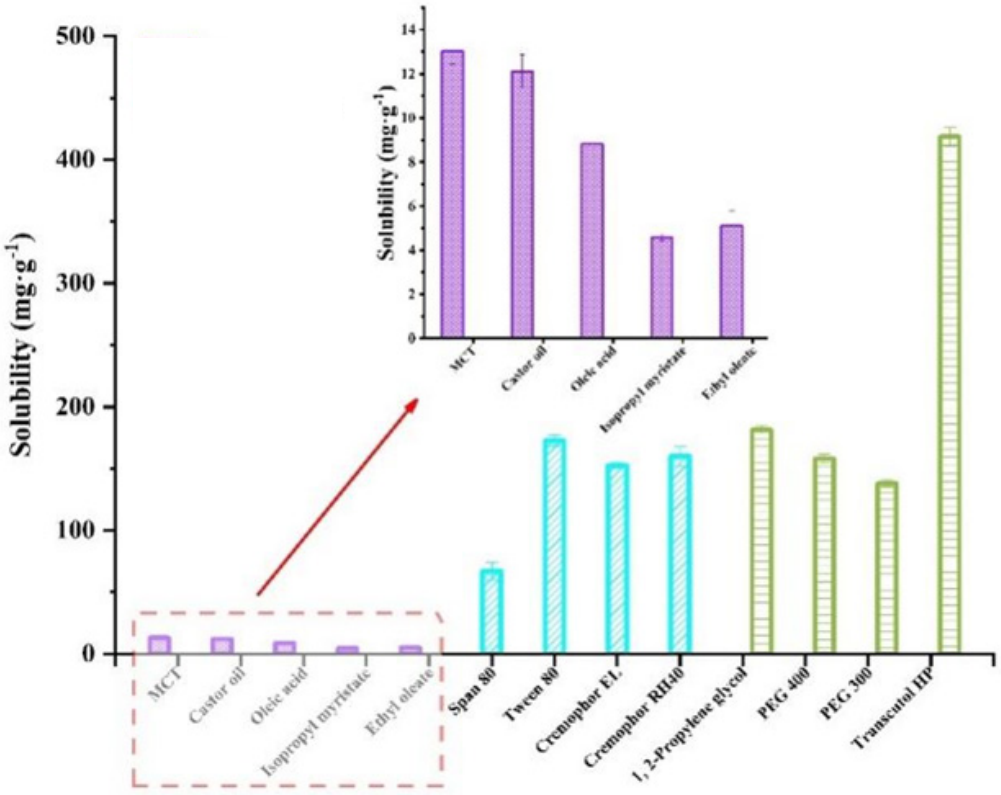

Fig. 2: Maximum solubility of celecoxib in various accessories (n=3)
Note: ( ): Oil; ( ): Emulsifier and ( ):Co-emulsifier

TABLE 1: COMPATIBILITY EXPERIMENT BETWEEN DIFFERENT OILS AND EMULSIFIERS

Oil	Emulsifiers	Oil:emulsifier				
		1:9	2:8	3:7	4:6	5:5
MCT	RH40	A	A	A	A	B
	EL35	A	A	A	B	B
	Tween 80	A	A	B	B	B
Oleic acid	RH40	A	A	A	B	D
	EL35	A	A	A	B	D
	Tween 80	B	C	E	E	E
Castor oil	RH40	A	A	A	B	B
	EL35	A	A	B	B	B
	Tween 80	A	B	B	B	B

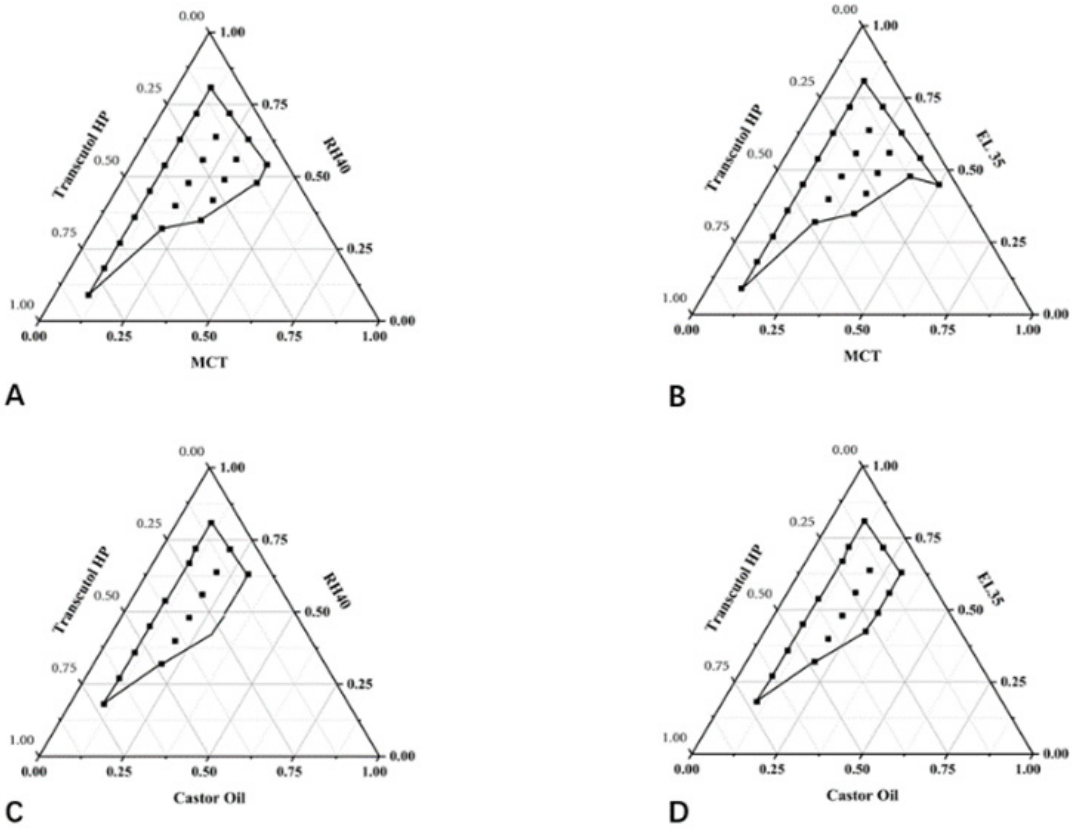

Fig. 3: Pseudo-ternary phase diagrams of different oil phases, emulsifiers and co-emulsifiers; (A) MCT (oil), RH40 (emulsifier) and Transcutol HP (co-emulsifier); (B) MCT (oil), EL35 (emulsifier) and Transcutol HP (co-emulsifier); (C) Castor oil (oil), RH40 (emulsifier) and Transcutol HP (co-emulsifier); and (D) Castro oil (oil), EL35 (emulsifier) and Transcutol HP (co-emulsifier

TABLE 2: EXPERIMENTAL VARIABLES AND LEVELS OF TEST VARIABLES

Factor	Level				
	-1.414	-1	0	1	1.414
W (oil)	10	14.3934	25	35.6066	40
Km	1	1.58579	3	4.41421	5

The three-dimensional effect surface (fig. 4) compared with Km showed that the W (oil) effect surface was steeper, which indicated that the oil had a greater influence on the light transmittance. The T % first increased and then decreased with the increase in W (oil) when Km was constant. Similarly, the T % first increased and then decreased as Km increased when W (oil) was constant. Finally, the optimal prescription was obtained and verified as W (oil) of 25 % with Km of 3.0. Thus, with 25.0 % oil, 56.25 % emulsifier and 18.75 % co-emulsifier, the model predicted that the T value of this prescription was 94.74 %.

The CXB-L-SMEDDS appeared as a light yellow clear transparent liquid which self-emulsified in water to form a uniform transparent microemulsion with a slightly blue light (fig. 5). CXB-L-SMEDDS formed small milk-like droplets with a diameter of about 22 nm after emulsification in water (fig. 6A). The results showed a relatively regular spherical shape which was consistent with the results of particle size of the formulation.

The particle size of the CXB-L-SMEDDS after the emulsification was about 22.68 nm, which was normally distributed, while the zeta potential was -31.92±0.24 mv with the Polydisperse Index (PDI) of 0.141 (fig. 6B). The smaller PDI value resulted in a narrower particle size distribution, which helped increased the oral bioavailability of the drug as seen in other studies[30]. Ideally, a zeta potential value of around ±30 mV was considered optimal for the physical stability of the emulsion[31]. The charge on the nanocarrier surface was one of the important factors that affected drug delivery through the lymphatic system, and negatively charged surfaces showed greater lymphatic transport compared to neutral or positively charged surfaces[32]. Therefore, it can be concluded that the optimal CXB-L-SMEDDS can form a uniform microemulsion system after emulsification.

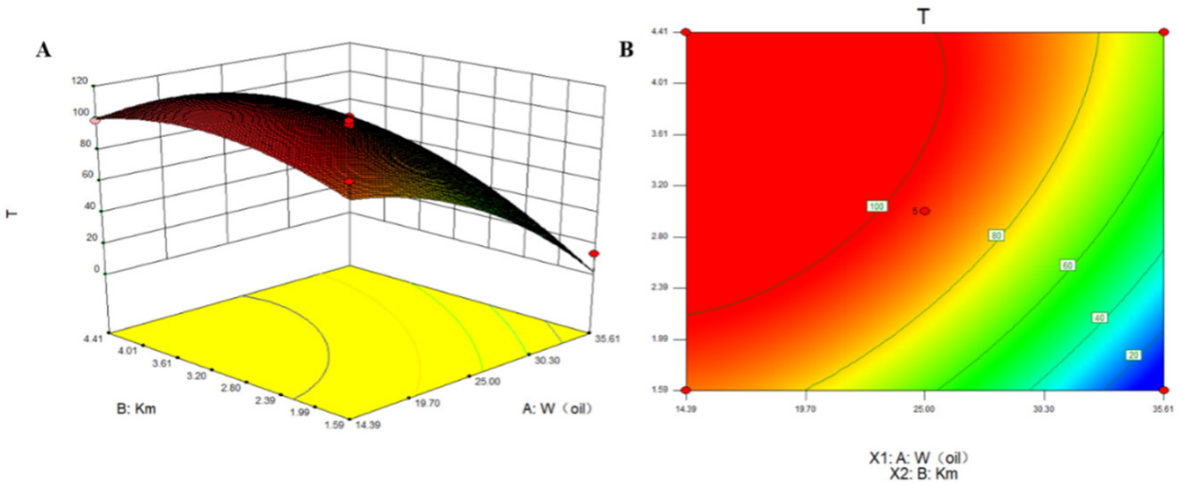

Fig. 4: Response surface model prediction; (A) 3-D response surface and (B) contour plot

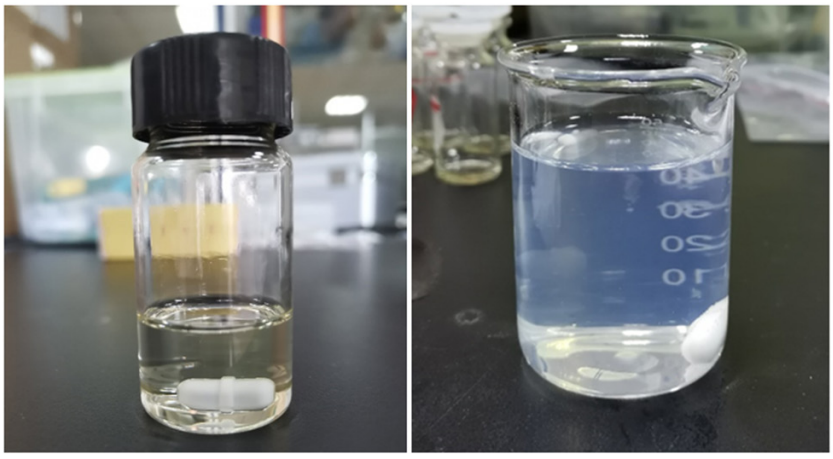

Fig. 5: The appearance of CXB-L-SMEDDS and microemulsion state

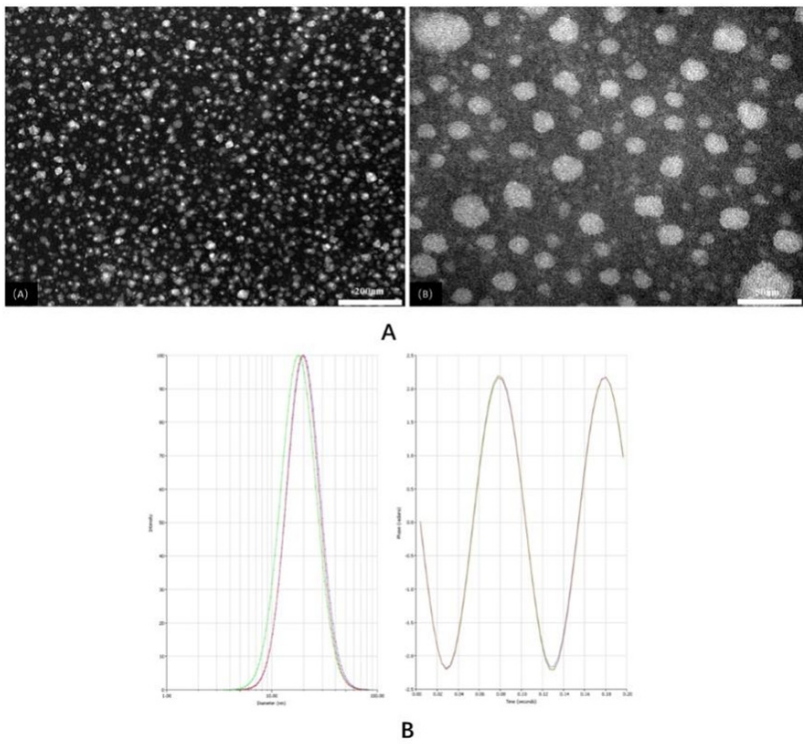

Fig. 6: (A) TEM image of CXB-L-SMEDDS emulsion forming microemulsion and (B) Particle size and zeta potential diagram of CXB-L-SMEDDS

The CXB-L-SMEDDS underwent three heating-cooling and freeze-thaw cycles with no change in appearance, and the microemulsion formed by self-emulsification did not delaminate, demulsify and precipitate drug crystals, which indicated that the formulation had good thermodynamic stability. The particle size of the microemulsion kept for 24 h still did not changed significantly, so the CXB-L-SMEDDS did not destroy the structure of the formed microemulsion after dilution in the gastrointestinal tract with different pH media (Table 3), and the formulation had good stability. The DL of CXB-L-SMEDDS was 10.17 % with EE of 97.65 %. The SD values were all less than 3 %, which indicated that the CXB-L-SMEDDS preparation process was stable and had good reproducibility. The appearance of CXB-L-SMEDDS did not change, and no delamination occurred at 4° and 30° for 60 d (Table 4). The particle size of microemulsion formed after emulsification was about 23 nm. However, the drug content was reduced over time (Table 4). The results showed that the prepared CXB-L-SMEDDS had good appearance stability within 60 d, but the drug content was reduced, so further curing was considered to improve the stability of CXB-L-SMEDDS.

Liquid microemulsion contains more surfactants which can significantly increase the solubility of poorly soluble drugs, but also stimulate the gastrointestinal tract to produce potential adverse reactions and cytotoxicity, so the biosafety of CXB-SMEDDS was investigated[33]. The CXB solution, CXB-SMEDDS and blank SMEDDS did not show significant cytotoxicity (fig. 7) in the dosage range of 20 to 200 $\mu g.ml^{-1}$ (the relative viability of the cells was above 75 %, and the cytotoxicity level was 0).

The adsorption capacity of water-insoluble adsorbent was significantly greater than that of water-soluble adsorbent with the maximum adsorption capacity of the solid adsorbent (Table 5). Neusilin-US2, Neusilin-UFL2, SYLOID®244 FP, anhydrous dicalcium phosphate, and Aeroperl®300 Pharma was selected as solid adsorbents for dissolution investigation, and the results showed that the release degree of anhydrous dicalcium phosphate>Neusilin-UFL2>Neusilin-US2>SYLOID®244 FP>Aeroperl®300 pharma (fig. 8). The solution in the dissolution cup showed clear and slightly blue light with no drug precipitation, and the drug precipitation crystals were only found in the dissolution experiment at 120 min. Water-soluble anhydrous dicalcium phosphate exhibited faster release, Aeroperl®300 Pharma had a high loading capacity and the prepared solid self-microemulsion also had very good fluidity.

However, the release degree was only about 40 % at 2 h, and the release was incomplete, which may be due to the medium and macroporous structure of Aeroperl®300 Pharma granules. The CXB-L-SMEDDS was adsorbed into the pores of the particles by capillary action, which resulted in dead adsorption. Neusilin-US2 is chemically magnesium aluminometasilicate that exists in solid state as mesoporous solids. The average particle size is 106 μm, and the surface area can reach 300 m^2/g. Since Neusilin-US2 is highly porous, the oil phase and surfactant penetrated into its pores rather than concentrated on the surface, so it was free to bind with the particles as stated in other reports[34]. According to the adsorption capacity, thus release degree and fluidity of solid microemulsion, Neusilin-US2 was selected as the solid adsorbent to prepare CXB solid microemulsion.

It was found that the fluidity, dissolution degree and particle size of the microemulsion formed after emulsification could not reach the best when Neusilin-US2 was used to prepare solid self-microemulsion with a maximum adsorption capacity of 2.5 g/g. So the ratio of CXB-L-SMEDDS and solid sorbent was screened. With the increase in the proportion, the fluidity of the powder was worse and the release degree of 120 min did not change much, but the particle size of the microemulsion obtained after emulsification gradually increased. Comprehensively considered, the ratio of CXB-L-SMEDDS and solid adsorbent was selected as 2:1.

TABLE 3: EFFECTS OF DIFFERENT DISPERSION MEDIA AND DILUTION RATIOS ON SELF-EMULSIFYING ABILITY OF CXB-L-SMEDDS

Physical characteristics	Degree of dilution in water			Media		
	1:50	1:100	1:200	pH 1.2	pH6.8	Water
Time (s)	30'62'	29'35'	28'83'	42'34'	32'04'	29'35'
T (%)	94.4	97	98.4	96.9	97	97
Leave for 24 h	93.4	96.5	97.3	96.3	95.8	96.5

TABLE 4: EFFECT OF TIME AND TEMPERATURE ON THE STABILITY OF CXB-L-SMEDDS (n=3)

Time (d)	Temperature (°)	Appearance	Particle size (nm)	Drug content ($mg \cdot g^{-1}$)
0	4	Uniform	22.5±0.4	98.11±0.21
	30	Uniform	23.2±0.3	100.01±0.13
30	4	Uniform	22.5±0.4	96.09±0.31
	30	Uniform	24.0±0.3	98.02±0.17
60	4	Uniform	23.5±0.7	92.15±0.38
	30	Uniform	23.8±0.3	89.22±0.34

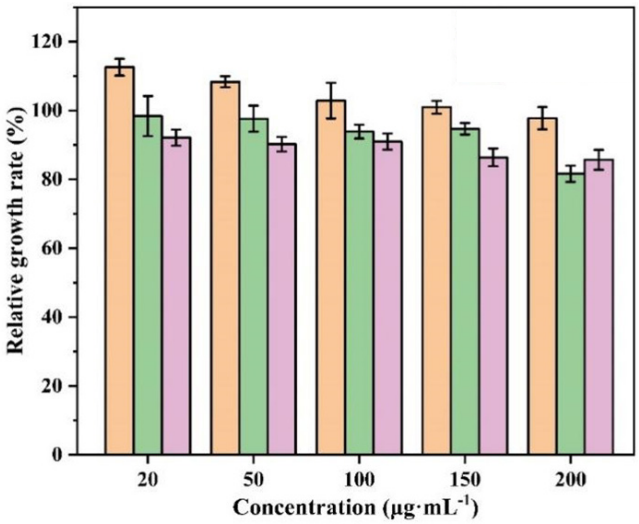

Fig. 7: Relative growth rate of Celecoxib, L-SMEDDS and CXB-L-SMEDDS (n=5)
Note: ( ): CXB; ( ): L-SMEDDS and ( ): CXB-L-SMEDDS

TABLE 5: MAXIMUM ADSORPTION CAPACITY OF EACH EXCIPIENT ON LIQUID FROM MICROEMULSION (n=3)

Species	Maximum adsorption capacity ($g \cdot g^{-1}$)	CI (%)	HR	Angle of repose (°)
Calcium Phosphate	0.68±2.60	25.74±1.34	1.33±1.15	48.26±2.07
Neusilin-UFL2	2.35±2.15	21.96±2.52	1.27±1.20	36.23±0.62
Neusilin-US2	2.49±1.50	15.48±4.29	1.19±1.46	35.59±2.28
Aeroperl®300 Pharma	1.84±0.67	22.42±2.04	1.37±2.17	30.89±1.41
Aerosil®200 Pharma	1.32±1.48	27.74±3.74	1.46±2.78	39.50±2.06
Mannitol	0.46±0.92	22.81±3.90	1.19±1.64	30.18±2.36
SYLOID®244 FP	2.15±0.61	32.97±1.53	1.37±0.85	37.61±2.25
Povidone K30	0.22±1.88	45.74±1.97	1.82±1.45	57.35±0.47

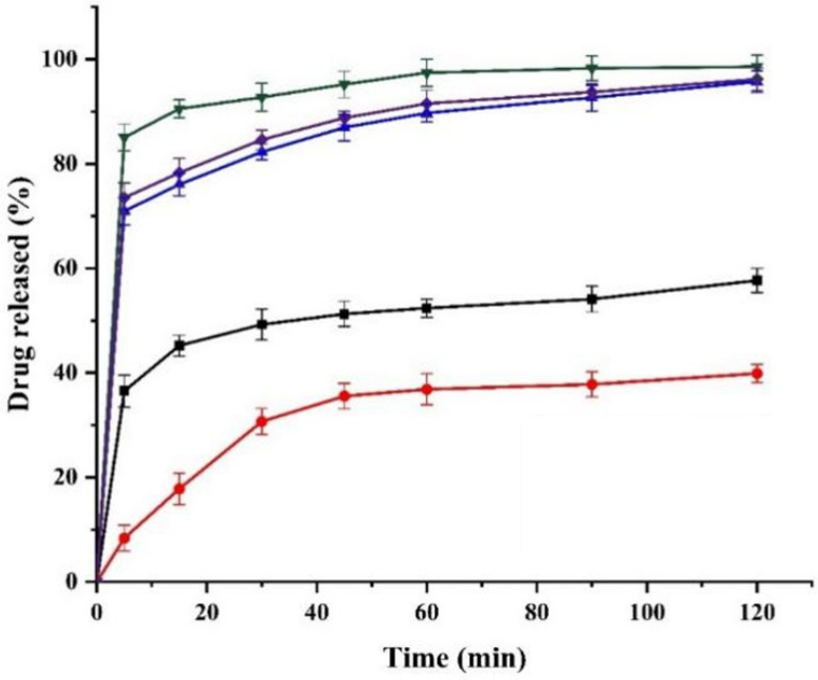

Fig. 8: Dissolution of different solid adsorbents (n=3)
Note: ( ): SYLOID® 244 FP; ( ): Acropcri®300 Pharma; ( ): Neusilin-US2; ( ): Calcium phosphate dibasic and ( ): Neusilin-UFL2

The results showed that the CXB Active Pharmaceutical Ingredient (API) had relatively regular bands or blocks with a relatively smooth crystal surface (fig. 9A and fig. 9B), but the Neusilin-US2 had a rough surface, high porosity, and relatively small powder particle size. The results showed CXB API in crystalline state and Neusilin-US2 with a rough surface granularity in the physical mixture of the two adsorbents (fig. 9C). The presence of CXB API crystal morphology was not observed in CXB-S-SMEDDS (fig. 9D), so it was inferred that CXB-L-SMEDDS had been adsorbed on the surface or pores of the solid adsorbent and existed in an amorphous form. The situation also led to an increase in CXB solubility, thereby improving the bioavailability of the drug.

The ME showed a slightly blue-light transparent emulsion, and the adsorbent precipitated to the bottom. The particle size of the microemulsion was 29.36±0.32 nm with the zeta value of -31.30±1.34 mv, and the PDI of 0.082±0.019, which indicated that the curing process did not destroy the self-emulsifying ability, and the formed ME had good stability.

XRD images showed the characteristic spikes representing the crystal structure of CXB (fig. 10), which indicated that the drug was in crystalline form. CXB API had obvious characteristic diffraction peaks, which also indicated that the crystal structure of the API was obvious. Neusilin-US2 had some low peaks, but no distinct

characteristic diffraction peaks, which had no effect on the peak shape of the drug. In contrast, there were no distinct diffraction peaks in CXB-S-SMEDDS, which indicated that the drug in the preparation had no crystal structure. Therefore, the drug existed in the molecular solubility state in CXB-S-SMEDDS, which effectively improved the solubility of the drug as stated in other studies [23].

The absorption peaks around 3338 and 3232 cm^{-1} were the N-H telescopic vibrations in the CXB -SO_2NH_2 group while the peaks around 1348 cm^{-1} were the S=O asymmetric telescopic vibrations in the CXB -SO_2NH_2 group (fig. 11). The absorption peaks around 1164 cm^{-1} were the S=O symmetrical telescopic vibrations in the CXB -SO_2NH_2 group while the peaks around 1230 cm^{-1} were the peaks generated by the C-F telescopic vibrations. The absorption peaks of the samples in CXB-S-SMEDDS significantly reduced the heterogeneous peaks, and the characteristic peaks of CXB disappeared, which indicated that CXB was almost completely adsorbed in the solid support as seen in other studies[35].

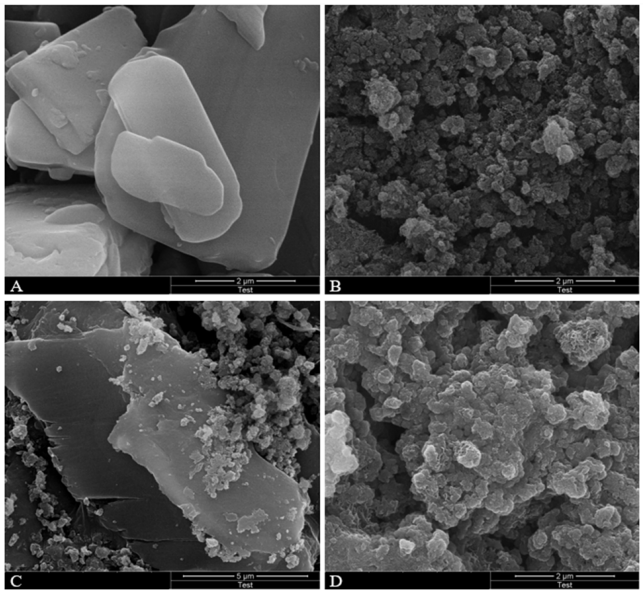

Fig. 9: The morphology of Celecoxib, Neusilin-US2, Physical mixture and CXB-S-SMEDDS; (A) SEM of Celecoxib powder; (B) SEM of Neusilin-US2 powder; (C) SEM of physical mixture powder; and (D) SEM of CXB-S-SMEDDS powder

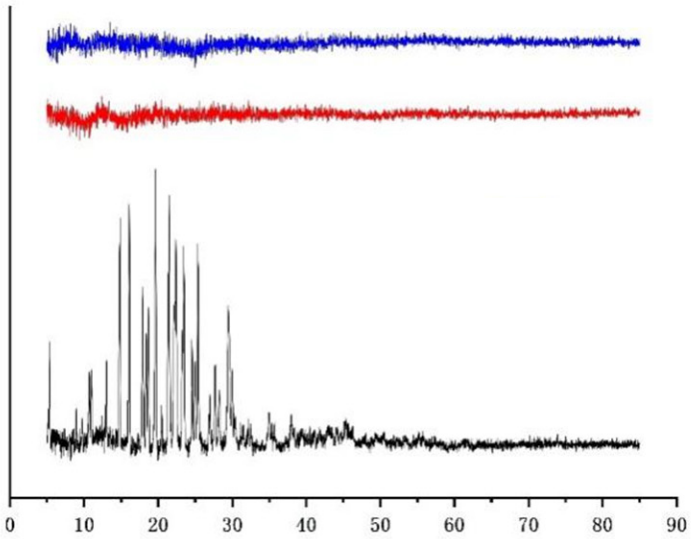

Fig. 10: X-ray diffraction pattern of different samples
Note: ( ): CXB-S-SMEDDS; ( ): Neusilin-US2 and ( ): Celecoxib

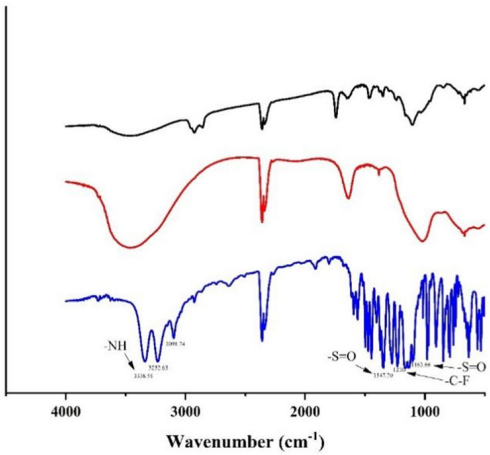

Fig. 11: Infrared spectra of celecoxib, CXB-S-SMEDDS and Neusilin-US2
Note: ( ): Celecoxib; ( ): Neusilin-US2 and ( ): CXB-S-SMEDDS

CXB had a sharp endothermic peak at 165.86° (fig. 12), which showed the crystalline properties of the drug used. The observation corresponded with the melting point of CXB as reported in the literature[36]. Therefore, it can be said that CXB was amorphous in solid self-emulsion and existed in amorphous form, thus, the physical state transition of CXB (from crystalline to amorphous) which was consistent with other reports[22].

The drug content of CXB-S-SMEDDS was 97.49±1.29 mg.g^{-1} which met the requirements of drug content uniformity. In the three release media, the release rates were as follows; CXB-L-SMEDDS>CXB-S-SMEDDS>CXB API (fig. 13). Thus, the cumulative release rates of the other samples were significantly higher than that of the CXB API. Under the conditions of HCl solution (pH of 1.2), PBS solution (pH of 6.8) and distilled water, the cumulative release rates of CXB-L-SMEDDS were 96.9 %, 98.3 % and 98.9 %, respectively, and that of CXB-S-SMEDDS were 92.3 %, 94.2 % and 96.2 %, respectively, while the cumulative release rates of CXB API were 3.87 %, 4.63 % and 2.49 %, respectively (fig. 12). Thus, the CXB API was almost not released. The results showed that the self-microemulsion technology significantly increased the cumulative release of the dissolution medium of CXB. After curing, the dissolution of CXB-S-S-SMEDDS was lower than that of CXB-L-SMEDDS. In addition, S-SMEDDS release was not affected by the pH of the dissolution medium. Thus, smaller particle size, larger surface area and spontaneous emulsification in contact with water make SMEDDS dissolve faster as stated in other reports[37].

Under the conditions of temperature of 40°±2° and relative humidity of 75 %±5 %, there was no obvious change in the appearance of CXB-S-SMEDDS, as well as no oil leakage and no change in the particle size after emulsification (Table 6). The results showed that the liquid had good stability after curing from the microemulsion.

Compared to CXB suspension (C_{max}=1031.1ng.ml^{-1}), the C_{max} of CXB-L-SMEDDS increased by 6.63-fold (6835.4 ng.ml^{-1}) and that of CXB-S-SMEDDS increased by 5.52-fold (5687.6 ng.ml^{-1}) (fig. 14 and Table 7). Similarly, compared with CXB (T_{max}=4 h), the T_{max} of CXB-L-SMEDDS was 3 h, but the T_{max} of CXB-S-SMEDDS was extended by 1 h. These results indicated that the SMEDDS increased the rate of *in vivo* drug absorption. Compared with the CXB suspension ($AUC_{0\text{-}24\ h}$=6370.9 ng.h.ml^{-1}) group, the $AUC_{0\text{-}24\ h}$ of the CXB-L-SMEDDS group and the CXB-S-SMEDDS group increased by 6.59-fold and 6.37-fold, respectively (41958.7 ng.h.ml^{-1} in the CXB-L-SMEDDS group and 40556.3 ng·h·ml^{-1} in the CXB-S-SMEDDS group), which also indicated that the SMEDDS significantly improved the bioavailability of CXB.

The pharmacokinetic results indicated that the SMEDDS improved the absorption and increased the bioavailability of CXB, which agreed with the results of the *in vitro* dissolution. The SMEDDS spontaneously formed O/W type microemulsions with a small particle size when it was released into the lumen of the Gastrointestinal Tract (GIT), so that lipophilic drugs remain in solution in the GIT. This condition was conducive to intestinal absorption and bioavailability of drugs as reported

by others[11]. In addition, the oil phase in SMEDDS increased the trans-lymphatic transport of drugs, and surfactants also increased the cross cellular permeability of the gastrointestinal membrane by disrupting the structural organization of the lipid bilayer, thereby improving bioavailability as seen in other studies[38].

In conclusion of this study, CXB SMEDDS were successfully developed using MCT, EL35 and Transcutol HP. The CCD design optimized the amount of oil, emulsifier and co-emulsifier in SMEDDS. Optimized L-SMEDDS prescription had smaller particle size and faster dissolution rate than API and also had a better safety profile. L-SMEDDS was solidified using solid carrier adsorption. S-SMEDDS prepared with Neusilin-US2 as adsorbent had the largest drug load, good fluidity and large release. X-ray, FT-IR, DSC characterization showed that CXB in S-SMEDDS existed in an amorphous form. This shift helped increase the drug release. Therefore, the *in vitro* releases of CXB-L-SMEDDS and CXB-S-SMEDDS were much higher than that of APIs. Pharmacokinetic studies showed that the L-SMEDDS and S-SMEDDS oral bioavailability were 6.59- and 6.37- folds higher than drug suspensions, respectively. In summary, this study developed optimized S-SMEDDS by solid carrier adsorption method to raise the bioavailability of CXB, solve the problems of poor long-term storage stability and interaction with capsule shell in L-SMEDDS, which was simple to prepare, low in economic cost and highly feasible for commercial production. Therefore, the S-SMEDDS can act as a promising formulation for a better oral delivery of CXB.

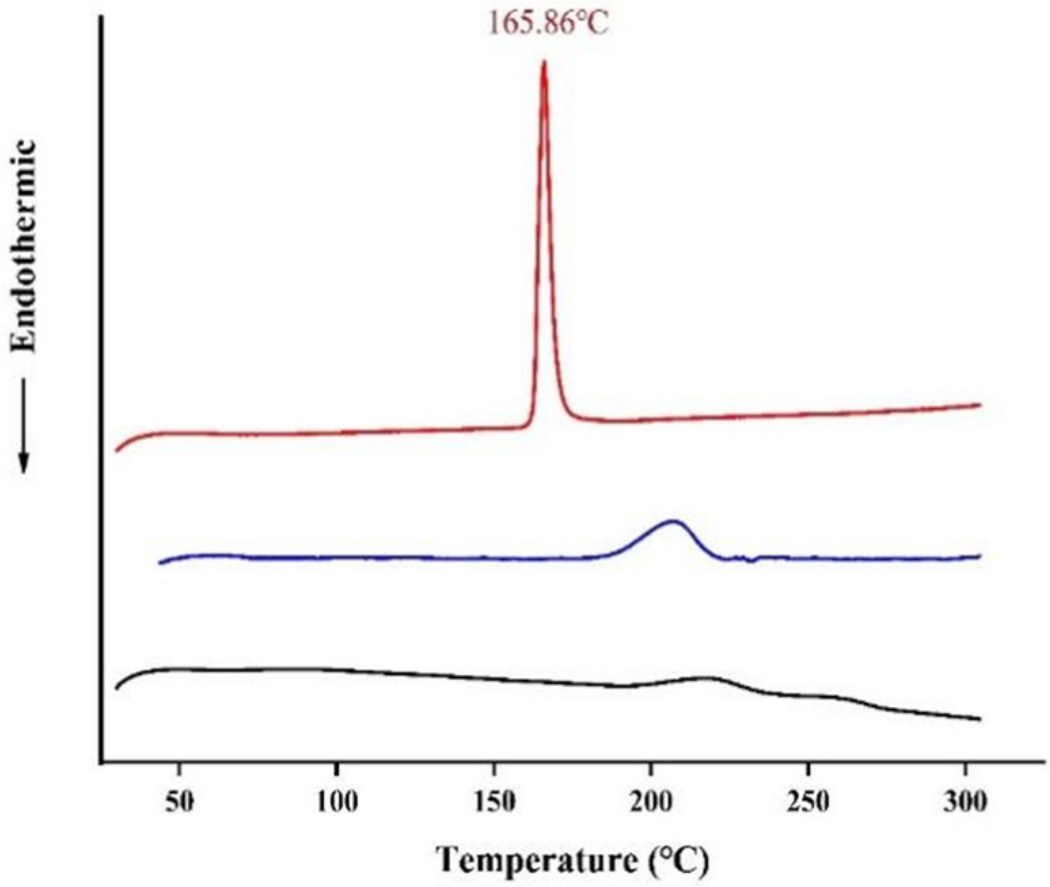

Fig. 12: DSC of Celecoxib, Neusilin-US2 and CXB-S-SMEDDS
Note: ( ): Neusilin-US2; ( ): Celecoxib and ( ): CXB-S-SMEDDS

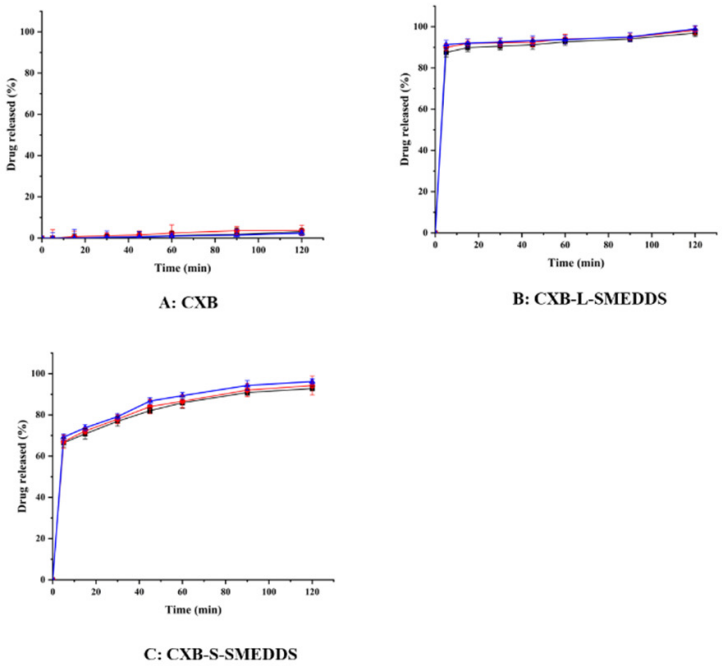

Fig. 13: ***In vitro*** **release curves of CXB, CXB-S-SMEDDS and CXB-L-SMEDDS**
Note: ( ): pH 1.2 HCl; ( ): pH 6.8 PBS and ( ): Water

TABLE 6: PRELIMINARY STABILITY TEST RESULTS (n=3)

Time(mo)	Appearance	Drug content ($mg \cdot g^{-1}$)
1	Uniform, no oil leakage	97.7±0.12
2	Uniform, no oil leakage	97.9±0.24
3	Uniform, no oil leakage	96.7±0.15
6	Uniform, no oil leakage	97.0±0.26

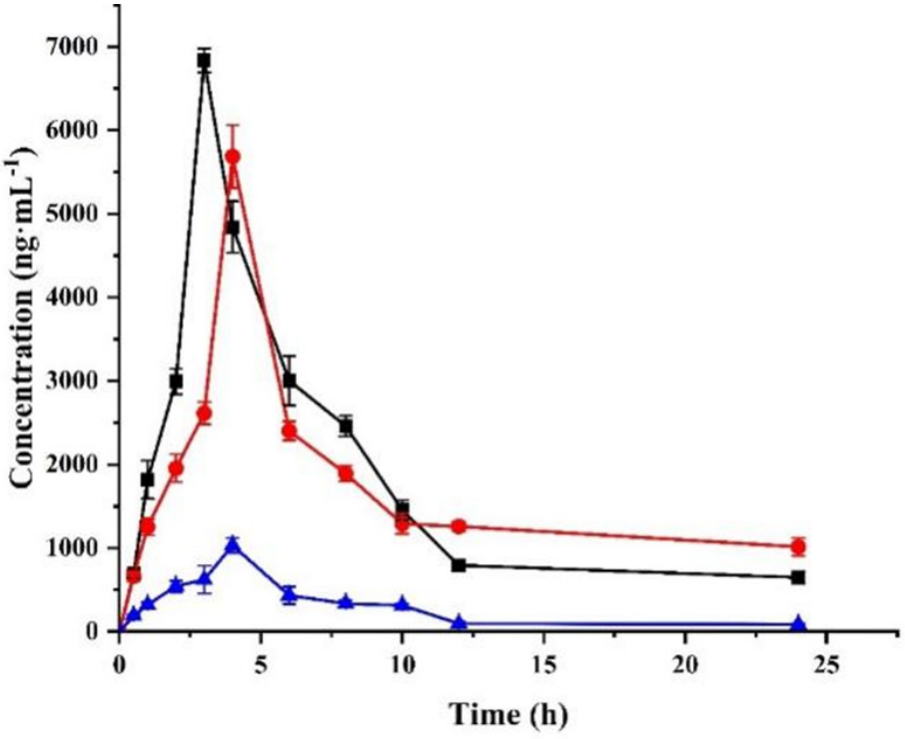

Fig. 14: Plasma drug concentration-time curve of Celecoxib API suspension, CXB-L-SMEDDS and CXB-S-SMEDDS (n=5)
Note: ( ): CXB-L-SMEDDS; ( ): CXB-S-SMEDDS and ( ): CXB

TABLE 7: PHARMACOKINETIC PARAMETERS OF CELECOXIB API SUSPENSION, CXB-L-SMEDDS AND CXB-S-SMEDDS

Parameter	Celecoxib	CXB-L-SMEDDS	CXB-S-SMEDDS
T_{max} (h)	4	3	4
C_{max} (ng.ml-1)	1031.1	6835.4	5687.6
$MRT_{0-\infty}$ (h)	10.8	7.7	51.6
$t_{1/2\alpha}$(h)	1.3	1.9	29.5
$t_{1/2B}$(h)	1.9	69.3	69.3
$AUC_{0-24\ h}$ (ng.h.ml^{-1})	6370.9	41958.7	40556.3
$AUC_{0-\infty}$(ng.h.ml^{-1})	7301.8	49602.2	98549.2

Conflict of interests:

No potential conflict of interest was reported by the authors.

Acknowledgments:

This work was supported by Wuyi University Scientific Research Project (No. 2017RC28; No. 2023AL001), 2021 Zhenjiang sixth "169 project" scientific research project, 2021 Jurong Social Development Science & Technology Program (No. ZA42109), Innovation and entrepreneurship project for returned overseas students in Jiangmen.

REFERENCES

1. Zhou S, Yang S, Huang G. Design, synthesis and bioactivities of Celecoxib analogues or derivatives. Bioorg Med Chem 2017;25(17):4887-93.
2. Hamed R, Omran H. Development of dual-release pellets of the non-steroidal anti-inflammatory drug celecoxib. J Drug Deliv Sci Technol 2020;55:101419.
3. Li JQ, Hao QY, Cao W, Vadgama JV, Wu Y. Celecoxib in breast cancer prevention and therapy. Cancer Manag Res 2018;10:4653-67.
4. He JL, Han Y, Xu GJ, Yin LF, Neubi MN, Zhou JP, *et al.* Preparation and evaluation of celecoxib nanosuspensions for bioavailability enhancement. RSC Adv 2017;7(22):13053-64.
5. Tran P, Nguyen TN, Park JS. Co-carrier-based solid dispersion of celecoxib improves dissolution rate and oral bioavailability in rats. J Drug Deliv Sci Technol 2023;79:104073.
6. Riahi MM, Sahebkar A, Sadri K, Nikoofal-Sahlabadi S, Jaafari MR. Stable and sustained release liposomal formulations of celecoxib: *In vitro* and *in vivo* anti-tumor evaluation. Int J Pharm 2018;540(1-2):89-97.
7. Nikam VK, Shete SK, Khapare JP. Most promising solid dispersion technique of oral dispersible tablet. Beni-Suef univ J Basic Appl Sci 2020;9:1-16.
8. Dhiman N, Sarvaiya J, Mohindroo P. A drift on liposomes to proliposomes: Recent advances and promising approaches. J Liposome Res 2022;32(4):317-31.
9. Song P, Tian Y, Hao G, Xu L, Sun Y, Sun Y. Preparation and evaluation of ibrutinib lipid-based formulations. J Drug Deliv Sci Technol 2022;77:103912.
10. Dokania S, Joshi AK. Self-Microemulsifying Drug Delivery System (SMEDDS)-challenges and road ahead. Drug Deliv 2015;22(6):675-90.
11. Karwal R, Garg T, Rath G, Markandeywar TS. Current trends in Self-Emulsifying Drug-Delivery Systems (SEDDSs) to enhance the bioavailability of poorly water-soluble drugs. Crit Rev Ther Drug Carr Syst 2016;33(1):1-39.
12. Ahn YS, Song JH, Kang BK, Kim MS, Cho SH, Rhee JM, *et al.* Preparation and characterization of liquefied ibuprofen using Self-Microemulsion Drug Delivery System (SMEDDS). J Pharm Investig 2004;34(1):35-42.
13. Liu HF, Mei JA, Xu Y, Tang L, Chen DQ, Zhu YT, *et al.* Improving the oral absorption of nintedanib by a self-microemulsion drug delivery system: Preparation and *in vitro*/*in vivo* evaluation. Int J Nanomed 2019;14:8739-51.
14. Wang YJ, Sun J, Zhang TH, Liu HZ, He FC, He ZG. Enhanced oral bioavailability of tacrolimus in rats by self-microemulsifying drug delivery systems. Drug Dev Ind Pharm 2011;37(10):1225-30.
15. Chen F, Huang G. Application of glycosylation in targeted drug delivery. Eur J Med Chem 2019;182:111612.
16. Zhang X, Huang G, Huang H. The glyconanoparticle as carrier for drug delivery. Drug Deliv 2018;25(1):1840-5.
17. Huang G, Huang H. Application of hyaluronic acid as carriers in drug delivery. Drug Deliv 2018;25(1):766-72.
18. Chen F, Huang G, Huang H. Preparation and application of dextran and its derivatives as carriers. Int J Biol Macromol 2020;145:827-34.
19. Huang S, Huang G. Design and application of dextran carrier. J Drug Deliv Sci Technol 2020;55:101392.
20. Silberstein S, Spierings EL, Kunkel T. Celecoxib oral solution and the benefits of Self-Microemulsifying Drug Delivery Systems (SMEDDS) technology: A narrative review. Pain Ther 2023;12(5):1109-19.
21. Bi X, Liu X, Di L, Zu Q. Improved oral bioavailability using a solid self-microemulsifying drug delivery system containing a multicomponent mixture extracted from *Salvia miltiorrhiza*. Molecules 2016;21(4):456.
22. Thota SK, Dudhipala N, Katla V, Veerabrahma K. Cationic solid SMEDDS of efavirenz for improved oral delivery: Development by central composite design, *in vitro* and *in vivo* evaluation. AAPS PharmSciTech 2023;24(1):38.
23. Madagul JK, Parakh DR, Kumar RS, Abhang RR. Formulation and evaluation of solid self-microemulsifying drug delivery system of chlorthalidone by spray drying technology. Dry Technol 2017;35(12):1433-49.

24. Midha K, Nagpall M, Singh G, Aggarwal G. Prospectives of solid self-microemulsifying systems in novel drug delivery. Curr Drug Deliv 2017;14(8):1078-96.
25. Schmied FP, Bernhardt A, Baudron V, Beine B, Klein S. Development and characterization of celecoxib Solid Self-Nanoemulsifying Drug Delivery Systems (S-SNEDDS) prepared using novel cellulose-based microparticles as adsorptive carriers. AAPS PharmSciTech 2022;23(6):213.
26. Deshmukh A, Kulkarni S. Solid self-microemulsifying drug delivery system of ritonavir. Drug Dev Ind Pharm 2014;40(4):477-87.
27. Omachi Y. Gastroretentive sustained-release tablets combined with a solid self-micro-emulsifying drug delivery system adsorbed onto fujicalin®. AAPS PharmSciTech 2022;23(5):157.
28. Sha K, Ma Q, Veroniaina H, Qi X, Qin J, Wu Z. Formulation optimization of solid self-microemulsifying pellets for enhanced oral bioavailability of curcumin. Pharm Dev Tech 2021;26(5):549-58.
29. Park SY, Jin CH, Goo YT, Chae BR, Yoon HY, Kim CH, *et al.* Supersaturable self-microemulsifying drug delivery system enhances dissolution and bioavailability of telmisartan. Pharm Dev Tech 2021;26(1):60-8.
30. Desai J, Thakkar H. Effect of particle size on oral bioavailability of darunavir-loaded solid lipid nanoparticles. J Microencapsul 2016;33(7):669-78.
31. Honary S, Zahir F. Effect of zeta potential on the properties of nano-drug delivery systems-a review (part 1). Trop J Pharm Res 2013;12(2):255-64.
32. Khan AA, Mudassir J, Mohtar N, Darwis Y. Advanced drug delivery to the lymphatic system: Lipid-based nanoformulations. Int J Nanomedicine 2013;8:2733-44.
33. Yeom DW, Chae BR, Son HY, Kim JH, Chae JS, Song SH, *et al.* Enhanced oral bioavailability of valsartan using a polymer-based supersaturable selfmicroemulsifying drug delivery system. Int J Nanomed 2017;12:3533-45.
34. Gumaste SG, Freire BO, Serajuddin AT. Development of solid SEDDS, VI: Effect of precoating of Neusilin (R) US2 with PVP on drug release from adsorbed self-emulsifying lipid-based formulations. Eur J Pharm Sci 2017;110:124-33.
35. Angi R, Solymosi T, Erdosi N, Jordan T, Karpati B, Basa-Denes O, *et al.* Preparation, pre-clinical and clinical evaluation of a novel rapidly absorbed celecoxib formulation. AAPS PharmSciTech 2019;20(2):90.
36. Jeon D, Kim KT, Baek MJ, Kim DH, Lee JY, Kim DD. Preparation and evaluation of celecoxib-loaded proliposomes with high lipid it content. Eur J Pharm Biopharm 2019;141:139-48.
37. Kumar D, Talegaonkar S, Bedi S, Dubey K. Design, development and evaluation of self-microemulsifying drug delivery system of pazopanib for enhanced dissolution rate and cytotoxic potential. J Drug Deliv Sci Technol 2023;80:104181.
38. Poudel BK, Marasini N, Tran TH, Choi HG, Yong CS, Kim JO. Formulation, characterization and optimization of valsartan self-microemulsifying drug delivery system using statistical design of experiment. Chem Pharm Bull 2012;60(11):1409-18.